Korean Journal of Ophthalmology 22(1):18-25, 2008
DOI : 10.3341/kjo.2008.22.1.18

Relationship between Scanning Laser Polarimetry with Enhanced Corneal Compensation and with Variable Corneal Compensation

Kyung Hoon Kim, MD[1], Jaewan Choi, MD[1,2], Chang Hwan Lee, MD[1],
Beom-Jin Cho, MD[2], Michael S. Kook, MD[1]

Department of Ophthalmology, University of Ulsan, College of Medicine, Asan Medical Center[1], Seoul, Korea
Hangil Eye Hospital[2], Incheon, Korea

***Purpose*:** To evaluate the structure-function relationships between retinal sensitivity measured by Humphrey visual field analyzer (HVFA) and the retinal nerve fiber layer (RNFL) thickness measured by scanning laser polarimetry (SLP) with variable corneal compensation (VCC) and enhanced corneal compensation (ECC) in glaucomatous and healthy eyes.
***Methods*:** Fifty-three eyes with an atypical birefringence pattern (ABP) based on SLP-VCC (28 glaucomatous eyes and 25 normal healthy eyes) were enrolled in this cross-sectional study. RNFL thickness was measured by both VCC and ECC techniques, and the visual field was examined by HVFA with 24-2 full-threshold program. The relationships between RNFL measurements in superior and inferior sectors and corresponding retinal mean sensitivity were sought globally and regionally with linear regression analysis in each group. Coefficients of the determination were calculated and compared between VCC and ECC techniques.
***Results*:** In eyes with ABP, R^2 values for the association between SLP parameters and retinal sensitivity were 0.06-0.16 with VCC, whereas they were 0.21-0.48 with ECC. The association of RNFL thickness with retinal sensitivity was significantly better with ECC than with VCC in 5 out of 8 regression models between SLP parameters and HVF parameters (P<0.05).
***Conclusions*:** The strength of the structure-function association was higher with ECC than with VCC in eyes with ABP, which suggests that the ECC algorithm is a better approach for evaluating the structure-function relationship in eyes with ABP.
Korean Journal of Ophthalmology 22(1):18-25, 2008

Key Words: GDx-ECC, GDx-VCC, Scanning laser polarimetry, Structure-function relationship

The loss of retinal ganglion cells in glaucoma leads to the localized or diffuse thinning of the retinal nerve fiber layer (RNFL), and its measurement has been correlated with visual field (VF) deficit.[1-3] In clinical practice, functional losses are usually assessed with standard automated perimetry. Structural losses may be assessed qualitatively (direct/indirect ophthalmoscopy, or red-free fundus photography) or more quantitatively (optical coherence tomography [OCT], scanning laser polarimetry [SLP], or confocal scanning laser ophthalmoscopy).[4,5] SLP with variable corneal compensation (GDx-VCC, Carl Zeiss Meditec, Inc., Dublin, CA) has become a widely used noninvasive clinical method for evaluating RNFL thickness in the detection of glaucomatous damage. The VCC technique was introduced to compensate individually for the true anterior segment retardation of each eye, which was not available in the original SLP devices with a fixed corneal compensator (FCC), and has been reported to be superior to SLP-FCC in terms of assessing the structure-function relationship, diagnostic accuracy, and higher interobserver and intraobserver reproducibilities.[6-11] However, the VCC technique sometimes produces images with an atypical birefringence pattern (ABP), which is characterized by retardation maps with alternating peripapillary circumferential bands of low and high retardation, variable areas of high retardation arranged in a spokelike peripapillary pattern, or splotchy areas of high retardation nasally and temporally, with a lower typical scan score (TSS).[6] It has been hypothesized

Received: May 28, 2007 *Accepted*: January 10, 2008
Reprint requests to Michael S. Kook, MD. Department of Ophthalmology, University of Ulsan, College of Medicine, Asan Medical Center. 388-1 Pungnap-2dong, Songpa-gu, Seoul 138-736, Korea. Tel: 82-2-3010-3677, Fax: 82-2-470-6440, E-mail: mskook@amc.seoul.kr

* This article was presented as a poster at the Association for Research in Vision and Ophthalmology annual meeting, April 30-May 4, 2006; Fort Lauderdale, Florida.

that such images are attributable to a low signal-to-noise ratio resulting from a diminution of reflectivity from the retinal pigment epithelium, which therefore increases the gain so as to augment the polarization signal, and paradoxically increases noise from deeper retinal structures such as the sclera.[6,12] It has been estimated that the overall prevalence of such images is 10-15%.[6,13,14] ABP may void the effect of custom compensation and provide spurious RNFL thickness measurements and result in reduced diagnostic ability of thickness parameters.[15] A support vector machine score or TSS provided by the imaging device has been reported to be highly predictive of ABP, with a high discriminating power between ABP and normal birefringence pattern (NBP).[6]

To reduce this biasing signal-to-noise ratio of VCC method, a new software-based compensation method-called the enhanced corneal compensation (ECC) algorithm-has recently been developed. The ECC algorithm (Carl Zeiss Meditec) deliberately introduces a known large birefringence bias into the measurement-beam path so as to shift the total retardation to a higher region; this is in contrast to the VCC method, in which SLP directly measures the relatively low RNFL retardation. The birefringence bias is determined from the macular region of each measurement, and is then mathematically removed point by point from the measured values to yield the actual RNFL retardation.[16] The ECC technique results in a polarization pattern that is significantly more typical than that obtained with the VCC technique, with the higher TSS value.[16-18] This means that ECC has a theoretical advantage over VCC in the neutralization of atypical polarization signals with high repeatability.[18]

Recent reports showed that better structure-function associations were achieved by the ECC algorithm than VCC with the analyses of 6 segmentation of RNFL areas and corresponding visual fields.[19,20] However, to our knowledge, no studies have investigated the association of a fairly larger areas of RNFL on the routine SLP printouts with corresponding retinal sensitivity in eyes grouped by their birefringence pattern, especially in eyes with ABP only. This study evaluated the relationship between global and regional SLP parameters measured by VCC and ECC and corresponding retinal sensitivity in eyes with ABP.

Materials and Methods

Twenty-eight eyes of 28 glaucomatous subjects and 25 eyes of 25 normal healthy subjects were enrolled in this prospective study. This study was approved by the institutional review board of the Asan Medical Center, and adhered to the tenets of the Declaration of Helsinki, with informed consent obtained from the subjects after the nature and possible consequences of the study were explained to them.

Subjects

Patients were recruited from December 2004 to April 2006 at the Asan Medical Center, Seoul, Republic of Korea, with the healthy subjects recruited from staff members, friends and spouses of patients, and volunteers. Each patient underwent a complete slit-lamp examination, central corneal thickness (CCT) measurement, visual field examination, and SLP measurements. CCT was measured three times by ultrasonic pachymetry (DGH-550, DGH Technology, Inc., Exton, PA) for all patients and the average was calculated.

For inclusion in the study, glaucomatous patients had to meet the following criteria: (1) typical glaucomatous optic nerve appearance; that is, focal or generalized narrowing or disappearance of the neuroretinal rim, disc hemorrhage, or the vertical cup-to-disc asymmetry of >0.2; (2) best-corrected visual acuity (BCVA) of 20/30 or better; and (3) reliable glaucomatous VF defects as detected in two consecutive fields obtained at least 2 months apart based on the 24-2 full-threshold program of a Humphrey VF analyzer (HVFA Ⅱ, Carl Zeiss Meditec, Inc.). The criteria for the presence of glaucomatous VF defects were as follows: a cluster of three points with a probability of <5% on a pattern deviation probability map in at least one hemifield, and including at least one point with a probability of <1%; a cluster of two points with a probability of <1%; a glaucoma hemifield test (GHT) result outside 99% of age-specific normal limits; and corrected-pattern standard deviation outside 95% of the normal limits. The affected eye was selected in glaucomatous patients with unilateral disease, and if both eyes of a patient showed glaucomatous change and met the inclusion criteria, one eye was randomly selected for entry.

All of the healthy control subjects had a BCVA of 20/30 or better, a normal and reliable VF, normal optic discs, and an intraocular pressure (IOP) of 21 mmHg or less. A VF was defined as normal when the GHT result was within normal limits and the field did not meet the above-listed criteria for a VF defect. Normal optic discs were defined as having intact neuroretinal rims, with no evidence of disc hemorrhage, notching, excavation, or asymmetry of the vertical cup-to-disc ratio of > 0.2. No other pathologic ocular condition other than mild age-related cataract was noted. One eye was selected randomly from healthy control subjects. Presence of ABP on the peripapillary SLP-VCC image was determined in masked fashion by one investigator (JC), and confirmed by using the software-provided TSS, which automatically calculates the degree of typicality between 0 and 100. For reference, the TSS ranges from 0 to 100, with lower scores associated with greater image atypia, and is applicable to both VCC and ECC images. ABP was defined as non-RNFL thickness based peripapillary polarisation, with TSS value <80, in accordance with previous reports.[13] The quality of each image included in the study was optimal (quality score $\geq$8). Finally, 53 eyes were classified as ABP (28 glaucomatous and 25 healthy controls).

Retinal Sensitivity Measurements

Retinal sensitivities were evaluated with the 24-2 HVFA full threshold program. A reliable VF was defined as having a false-positive error rate of <33%, a false-negative error rate of <33%, and a fixation loss of <20%. The retinal mean sensitivity (MS) was expressed in two forms: in dB and unlogged 1/Lambert (L) scales. The differential light sensitivity (DLS) at each tested location was measured according to DLS (dB)=$10\times\log_{10}$ [$L_{max}/(L_t-L_b)$], where L_{max} is the maximal stimulus luminance, L_t is the stimulus luminance at threshold, and L_b is the background luminance. For simplicity, this relationship can be written as $10\times\log_{10}$ ($1/L$). The unlogged $1/L$ at each tested location was calculated by dividing the dB value by 10 and then calculating the reverse logarithm; the average value was then evaluated. No adjustment was made for the type of thresholding algorithm used. Two test points adjacent to the blind spot were excluded from the analysis.

The global MS was defined as the average overall value of the DLS obtained at each test point. The regional MS was defined as the following. We detailed the VF sensitivity map corresponding to superior or inferior RNFL sectors along the 120° sectors on SLP, on the basis of the article by Garway-Heath et al.[21] To be specific, we excluded the VF test points corresponding to nasal 70° and temporal 50° RNFL sectors. Superior retinal MS corresponding to the inferior 120° RNFL sectors was calculated from the remaining 25 test points in superior hemifield, and inferior retinal MS corresponding to superior 120° RNFL sectors was calculated from the remaining 22 test points in inferior hemifield (Fig. 1).

Scanning Laser Polarimetry Measurements

SLP images were obtained with a GDx-VCC system (software version 5.5.0). The instrument works both with VCC and (in a special research-mode version) with ECC. In our investigation, SLP measurements with both VCC and ECC techniques were performed on each eye during the same session. Image acquisition was performed in all subjects with eyes undilated. The experimental preparation protocol and the image acquisition procedure have been described in detail elsewhere.[9,22] In brief, after the refractive error of each eye was entered into the software to allow sharp focus on the retina, patients were instructed to maintain their heads as vertically as possible in the face mask of the GDx-VCC instrument so as to ensure consistent alignment. The anterior segment birefringence was assessed in each eye. Adequate compensation of the anterior segment birefringence was verified subjectively by looking at the retardation pattern in the macular region. A baseline image was automatically created from averaging three images obtained for each eye. All accepted images exhibited a centered optic disc, were well-focused with even and adequate illumination, and had no motion artifacts. The margin of the optic disc was manually marked with an ellipse on a reflectance image of the fundus. The software automatically positioned a circle with a width of 8 pixels corresponding to approximately 2.3 mm on the center of the drawn ellipse. Based on the retardation values within this area, the software calculated the following parameters: TSNIT (temporal, superior, nasal, inferior, and temporal) average, superior average, inferior average, TSNIT standard deviation (SD), inter-eye symmetry, and nerve fiber indicator (NFI). The inter-eye symmetry,

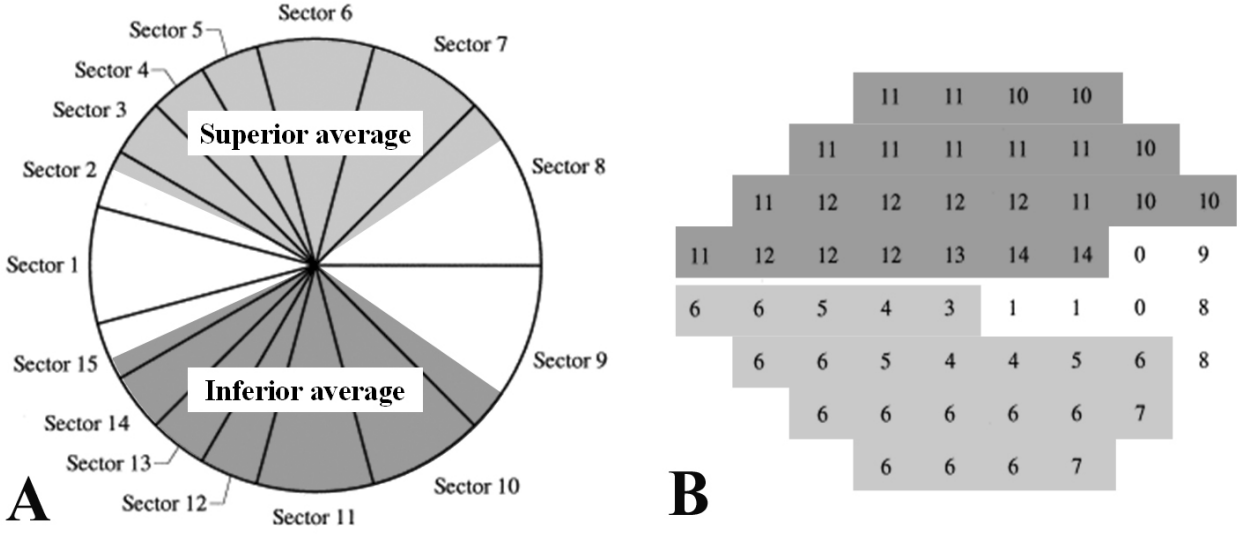

Fig. 1. Correspondence map of the GDx-VCC regional parameters (A) and the HVFA 24-2 paradigm (B) for a right eye. In the present study, peripapillary GDx-VCC measurements and visual field test points were grouped into two regional corresponding sectors of superior and inferior average on the GDx-VCC printouts, based on the article by Garway-Heath et al.[21] Corresponding sectors were grayscaled and named after the parameters on the GDx-VCC printouts (Superior and inferior average) in relation to the optic disc.

which describes the correlation in the retardation measurements between the eyes of a subject, and NFI, which describes the likelihood of glaucoma as calculated by an artificial neural network based on the normative database stored in the device, were not used in the analysis because only one eye from each subject was used and the appropriate normative database was not available for the ECC software.

On the routine GDx-VCC printouts, the peripapillary measurement circle is divided into temporal 50° sector, nasal 70° sector, and two equally sized sectors of superior and inferior 120° sectors. Superior and inferior average reflect regional mean RNFL thickness values along the regional 120° sectors of superior and inferior peripapillary hemicircle. In contrast, TSNIT average reflects mean RNFL thickness values along the whole 360° sectors of the peripapillary circle, and TSNIT SD reflects the modulation of the double-hump pattern derived from the whole sectors. These two parameters were considered as global SLP parameters.

Statistical Analysis

Descriptive statistics (number and percentage for categorical variables, and mean±SD for continuous variables) including VF parameters and SLP parameters (VCC and ECC techniques) were initially evaluated for each group. The Mann-Whitney U test was applied to continuous variables to assess differences between glaucomatous and healthy eyes in each group. The Wilcoxon signed ranks test was used for SLP parameters to assess differences between VCC and ECC parameters.

We sought the association of TSNIT average and TSNIT SD values with the global MS in dB and unlogged 1/*L* scale. Superior and inferior average was associated with inferior MS and superior MS, respectively. These relationships between SLP parameters measured by VCC and ECC and retinal sensitivity were evaluated with linear ($y=a+bx$) regression analysis. In linear regression analysis, the goodness-of-fit of any particular regression model is expressed as the coefficient of determination, R^2, which indicates the proportion of the total variation in the dependent variable accounted for by the regression function. To compare the strength of association between VCC and ECC, the absolute prediction errors (absolute values of the residuals) from each model were compared by Wilcoxon signed ranks tests.[23] Differences with a probability value of $P<0.05$ were considered statistically significant.

Results

Table 1 presents the patient demographics and biometric parameters including VF and SLP data in eyes with ABP. Age, spherical equivalent (SE), and CCT did not differ between glaucomatous and normal eyes. IOP was higher in the glaucomatous eyes than in normal ones ($P=0.002$).

Table 1. Descriptive statistics for demographics and clinical characteristics of the study patients

	Eyes with ABP		
	Glaucomatous (n=28)	Normal (n=25)	*P*-value
Age	62.5±12.7	58.0±14.1	ns
Gender (M:F)	22:6	8:17	ns
SE	-2.5±2.9	-2.4±3.2	ns
IOP	16.5±4.4	14.6±3.0	0.002*
CCT	526.5±41.6	543.9±21.7	ns
Visual field parameters and retinal sensitivity (dB)			
MD	-11.6±7.1	-2.6±2.7	<0.001*
PSD	9.0±3.6	2.2±1.3	<0.001*
Global MS	16.9±6.9	26.8±5.7	<0.001*
Superior MS	15.0±8.3	26.3±5.9	<0.001*
Inferior MS	19.3±8.1	27.4±5.7	<0.001*
SLP parameters: VCC (ECC)			
TSNIT average	45.0±7.3 (40.7±8.4)†	54.3±10.2 (50.5±6.5)†	<0.001* (<0.001*)
Superior average	50.4±10.6 (49.0±12.3)	62.8±9.8 (61.0±8.0)	<0.001* (<0.001*)
Inferior average	45.8±7.9 (48.0±9.6)	59.6±11.3 (60.6±13.9)	<0.001* (<0.001*)
TSNIT standard deviation	13.0±5.7 (16.2±4.5)†	17.5±4.6 (22.3±4.0)†	<0.001* (<0.001*)
TSS	57 (100)‡	61 (100)‡	*ns* (*ns*)

Data are mean±SD values, except for TSS (median value). *$P<0.05$, independent samples *t*-test between glaucomatous and normal eyes; †$P<0.05$, paired *t*-test between VCC and ECC; ‡$P<0.05$, Wilcoxon signed ranks test between VCC and ECC. Abbreviations: ABP=atypical birefringence pattern; SE=spherical equivalent; IOP=intraocular pressure; CCT=central corneal thickness; dB=decibel; MD=mean deviation; PSD=pattern standard deviation; MS=mean sensitivity; SLP=scanning laser polarimetry; VCC=variable corneal compensation; ECC=enhanced corneal compensation; TSNIT=temporal, superior, nasal, inferior and temporal; TSS=typical scan score.

Table 2. Linear regression analyses between SLP parameters and retinal sensitivity expressed in the dB and 1/*L* scales

		Eyes with ABP (n=53)		
		GDx-VCC	GDx-ECC	
SLP parameter	HVF parameter	R^2 (*P*-value)	R^2 (*P*-value)	*P*-value
TSNIT average	Global MS (dB)	0.07 (0.06)	0.25 (<0.001*)	0.079
	Global MS (1/*L*)	0.06 (0.08)	0.21 (<0.001*)	0.36
TSNIT standard deviation	Global MS (dB)	0.10 (0.02*)	0.37 (<0.001*)	0.001†
	Global MS (1/*L*)	0.14 (0.007*)	0.33 (<0.001*)	0.041†
Superior average	Inferior MS (dB)	0.06 (0.07)	0.24 (<0.001*)	0.002†
	Inferior MS (1/*L*)	0.13 (0.007*)	0.27 (<0.001*)	0.006†
Inferior average	Superior MS (dB)	0.16 (0.003*)	0.48 (<0.001*)	<0.001†
	Superior MS (1/*L*)	0.16 (0.003*)	0.25 (<0.001*)	0.21

* $P<0.05$, linear regression; † $P<0.05$, Wilcoxon signed ranks test of absolute prediction errors between VCC and ECC.
Abbreviations: SLP=scanning laser polarimetry; dB=decibel; *L*=Lambert; ABP=atypical birefringence pattern; MS=mean sensitivity.

There were statistically significant differences between glaucomatous and normal eyes in all VF parameters and SLP parameters except for TSS, either with VCC or ECC ($P<0.001$). TSNIT SDs were consistently higher with ECC than with VCC ($P<0.001$). TSS was higher with ECC than with VCC ($P<0.05$, Wilcoxon signed ranks test). For instance, the median TSS values were 57 with VCC and 100 with ECC in glaucomatous eyes, and 61 with VCC and 100 with ECC in normal eyes ($P<0.001$). The relationships between VCC and ECC parameters and retinal sensitivities are presented in Table 2. In eyes with ABP, R^2 values were significantly higher with ECC than with VCC for 5 out of 8 comparison models. All regression models between TSNIT SD and retinal sensitivities and between superior average and inferior MS had significantly higher R^2 values with ECC than with VCC ($P<0.05$). The model between inferior average and superior MS (dB) had significantly higher R^2 value with ECC than with VCC ($P<0.001$).

Fig. 2 shows the examples of structure-function relationship between VCC and ECC measurements [TSNIT SD, superior average and inferior average] and retinal sensitivity expressed in dB scale by linear regression in eyes with ABP. All regression models showed statistical significances ($P<0.05$) except for the model, which is superior average with VCC versus inferior MS ($P=0.07$), and R^2 values were significantly higher for linear associations of these SLP parameters with retinal sensitivity with ECC than with VCC (*P*-values: A, 0.001; B, 0.002; C, <0.001. Wilcoxon signed ranks test of the absolute prediction errors).

Discussion

Elucidating the structure-function relationship in glaucoma represents an effective method for understanding the course of the disease and for validating the diagnostic accuracy of the new optical imaging algorithm of SLP. In this cross-sectional study, the associations between VCC and ECC measurements and retinal sensitivity were analyzed based on the default four-sector classification of the peripapillary RNFL area on the SLP printouts and retinal sensitivity expressed in dB and unlogged 1/*L* scales of the corresponding VF. The parameters employed in the present study to represent the global and regional RNFL damage were the following: TSNIT average, superior average, inferior average, and TSNIT SD. Since TSNIT SD indicates the modulation of the double-hump pattern derived from the whole sectors, we regarded it as a reasonable surrogate indicator of underlying structural damage, and included it as an independent global SLP parameter in the analysis. A lower value reflects more advanced structural RNFL attenuation along the superior and inferior quadrants. Applying these feasible parameters on the printouts could provide practical data in the standard clinical settings. In addition, some studies have found low correlations between the VCC RNFL thickness in the nasal and temporal sectors and the corresponding visual sensitivity.[1,3,20,24] The lack of a relationship in these areas has been explained by the lower amounts of retardation relative to that measured in other sectors resulting in a low signal-to-noise ratio, which possibly obscures a correlation with poor polarimetric reproducibility.

Our method was derived from looking at relatively larger areas of RNFL and corresponding visual field, when compared with the recent publications.[19,20] To make up for this problem, we looked into our visual field data with more detail on the basis of the article by Garway-Heath et al.[21], which provides the basis of mapping the visual field to the optic disc for the most of the articles dealing with structure-function relationships. Because of the fixed dimensions of the SLP printouts, the size and orientation of the optic nerve head quadrants differed slightly from the original article, but were nearly consistent with their published relationship between optic nerve head location and visual field test points.

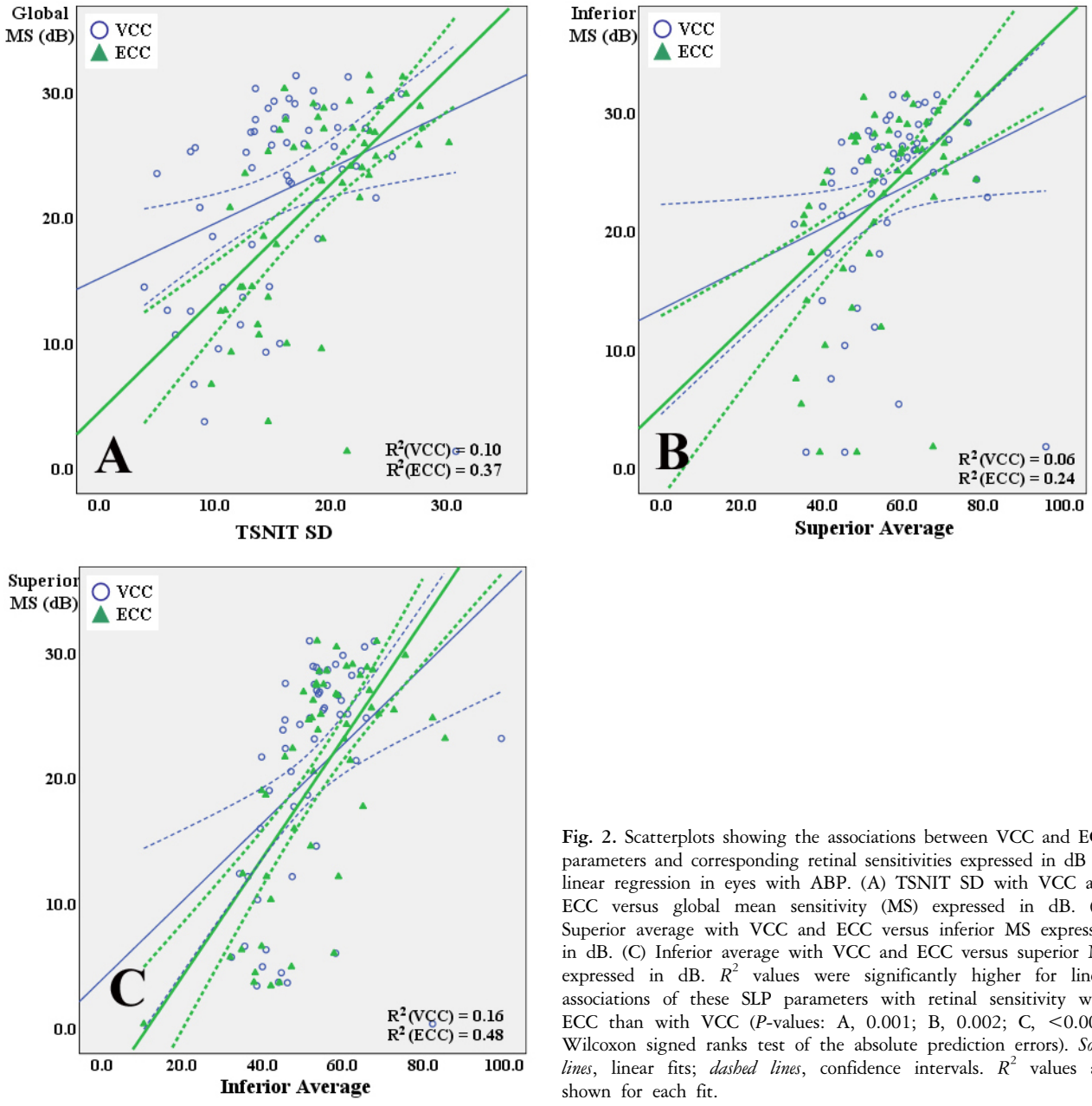

Fig. 2. Scatterplots showing the associations between VCC and ECC parameters and corresponding retinal sensitivities expressed in dB by linear regression in eyes with ABP. (A) TSNIT SD with VCC and ECC versus global mean sensitivity (MS) expressed in dB. (B) Superior average with VCC and ECC versus inferior MS expressed in dB. (C) Inferior average with VCC and ECC versus superior MS expressed in dB. R^2 values were significantly higher for linear associations of these SLP parameters with retinal sensitivity with ECC than with VCC (*P*-values: A, 0.001; B, 0.002; C, <0.001. Wilcoxon signed ranks test of the absolute prediction errors). *Solid lines*, linear fits; *dashed lines*, confidence intervals. R^2 values are shown for each fit.

In eyes with ABP, 5 out of 8 regression models showed significantly better structure-function associations with ECC than with VCC ($P<0.05$). As ECC can potentially improve polarimetric image analysis of RNFL in eyes with ABP in previous reports,[13,18] we hypothesized that the evaluation of the structure-function relationship may also be enhanced with this novel software algorithm. In detail, the error in measurements introduced by atypical retardation when using the VCC in eyes with ABP might artifactually increase the apparent RNFL thickness throughout the retina, and significantly weakens the correlation with retinal sensitivity.

Bowd et al.[19] showed that the RNFL thinckness associations with VF sensitivity generally were slightly stronger for ECC than for VCC, although these differences were only significant for inferotemporal RNFL. Mai et al.[20] showed that correlations in the structure-function relationship were generally stronger in images taken with ECC than in those taken with VCC. However, no statistical significances were found in the structure-function relationship between VCC and ECC, when eyes with marked ABP images were removed from the analysis. Our study is different from their reports in that we have investigated the association of a fairly larger areas of RNFL with corresponding retinal sensitivity in eyes with ABP, which could weaken the structure-function relationship.

Interestingly, the differences between VCC and ECC were

distinct in the association of TSNIT SD with retinal sensitivity in eyes with ABP. All association models between TSNIT SD and global retinal sensitivity revealed statistical significance between VCC and ECC (P<0.05). Our explanation for these results is that reducing nasal and temporal atypical birefringence with ECC algorithm enhances the true pattern of RNFL distribution in eyes with ABP, resulting in the more accurate TSNIT SD value and the better association with retinal sensitivity.

The ECC algorithm showed better association than VCC in models associated with superior average and retinal sensitivities and in model associated with inferior average and superior MS (dB).

GDx-VCC has exhibited limited efficacy in evaluations of the RNFL status of the eyes with ABP (i.e., high myopic eyes, eyes with retinal pigment epithemium atrophy, and in some emmetropic glaucomatous eyes).[12,14,25] Uncertainties in interpretations of RNFL status in these eyes adversely affect the discriminating power of GDx-VCC, leading to false judgments in clinical situations. Da Pozzo et al. suggested that ABP voids the effect of custom compensation and provides spurious RNFL thickness measurements, and that when evaluating a printout with ABP, it is better to rely on ratios, modulation parameters, and NFI than on SLP thickness parameters, since the diagnostic ability of thickness parameters is significantly reduced.[15] Our data demonstrate that there is a better association between retinal sensitivities and SLP parameters derived from the ECC algorithm than those derived from the established VCC algorithm in eyes with ABP. However, it should be noted that better structure-function association of ECC does not necessarily mean superior diagnostic ability on structural damage over VCC.

Selection bias may have the potential to affect the apparent structure-function relationship in this study. Glaucomatous and healthy eyes were recruited based on the VF loss, without requirements for structural RNFL damage. Because the selection criteria were based on the VF damage, it is possible that patients with VF loss, but without any structural RNFL damage, are included. This kind of selection bias might work in the direction that functional damage appears more advanced than the actual structural change. The regional topography used for SLP in this study was based on the basic parameters on the SLP printouts, and the corresponding retinal sensitivity was calculated in somewhat different way from the previous articles. The relatively larger SLP and corresponding VF areas in our study might not represent the optimal combination for evaluating the structure-function relationship. However, no definitive structure-versus-function map has been accepted as a gold standard, and the ultimate aim of our study was to illustrate and compare the degree of structure-function association derived from the default SLP settings with the different algorithms in standard clinical settings.

In conclusion, this new software-based ECC algorithm seems to be effective in evaluating the structure-function relationship in eyes with ABP, as well as it could reduce the atypical birefringence.

References

1. Reus NJ, Lemij HG. The relationship between standard automated perimetry and GDx-VCC measurements. *Invest Ophthalmol Vis Sci* 2004;45:840-5.
2. Lan YW, Henson DB, Kwartz AJ. The correlation between optic nerve head topographic measurements, peripapillary nerve fiber layer thickness, and visual field indices in glaucoma. *Br J Ophthalmol* 2003;87:1135-41.
3. Schlottmann PG, De Cilla S, Greenfield DS, et al. Relationship between visual field sensitivity and retinal nerve fiber layer thickness as measured by scanning laser polarimetry. *Invest Ophthalmol Vis Sci* 2004;45:1823-9.
4. Greenfield DS. Optic nerve and retinal nerve fiber layer analyzers in glaucoma. *Curr Opin Ophthalmol* 2002;13: 68-76.
5. Blumenthal EZ, Weinreb RN. Assessment of the retinal nerve fiber layer in clinical trials of glaucoma neuroprotection. *Surv Ophthalmol* 2001;45(Suppl 3):S305-12.
6. Bagga H, Greenfield DS. Quantitative assessment of structural damage in eyes with localized visual field abnormalities. *Am J Ophthalmol* 2004;137:797-804.
7. Zhou Q, Weinreb RN. Individualizd compensation of anterior segment birefringence during scanning laser polarimetry. *Invest Ophthalmol Vis Sci* 2002;43:2221-8.
8. Weinreb RN, Bowd C, Zangwill LM. Glaucoma detection using scanning laser polarimetry with variable corneal polarization compensation. *Arch Ophthalmol* 2003;121: 218-24.
9. Kook MS, Cho HS, Seong M, Choi J. Scanning laser polarimetry using variable corneal compensation in the detection of glaucoma with localized visual field defects. *Ophthalmology* 2005;112:1970-8.
10. Frenkel S, Slonim E, Horani A, et al. Operator learning effect and interoperator reproducibility of the scanning laser polarimeter with variable corneal compensation. *Ophthalmology* 2005;112:257-61.
11. Lleo-Perez A, Ortuno-Soto A, Rahhal MS, et al. Intraobserver reproducibility of retinal nerve fiber layer measurements using scanning laser polarimetry and optical coherence tomography in normal and ocular hypertensive subjects. *Eur J Ophthalmol* 2004;14:523-30.
12. Bozkurt B, Irkec M, Gedik S, et al. Effect of peripapillary chorioretinal atrophy on GDx parameters in patients with degenerative myopia. *Clin Experiment Ophthalmol* 2002;30: 411-4.
13. Tóth M, Holló G. Enhanced corneal compensation for scanning laser polarimetry on eyes with atypical polarisation pattern. *Br J Ophthalmol* 2005;89:1139-42.
14. Hoh ST, Greenfield DS, Liebmann JM, et al. Factors affecting image acquisition during scanning laser polarimetry. *Ophthalmic Surg Lasers* 1998;29:545-51.
15. Da Pozzo S, Marchesan R, Canziani T, et al. Atypical pattern of retardation on GDx-VCC and its effect on retinal nerve fiber layer evaluation in glaucomatous eyes. *Eye* 2006;20:767-75.
16. Tóth M, Holló G. Evaluation of enhanced corneal compensation in scanning laser polarimetry: comparison with variable corneal compensation on human eyes undergoing LASIK. *J Glaucoma* 2006;15:53-9.
17. Reus NJ, Zhou Q, Lemij HG. Enhanced imaging algorithm

for scanning laser polarimetry with variable corneal compensation. *Invest Ophthalmol Vis Sci* 2006;47:3870-7.
18. Sehi M, Guaqueta DC, Greenfield DS. An enhancement module to improve the atypical birefringence pattern using scanning laser polarimetry with variable corneal compensation. *Br J Ophthalmol* 2006;90:749-53.
19. Bowd C, Tavares IM, Medeiros FA, et al. Retinal Nerve Fiber Layer Thickness and Visual Sensitivity Using Scanning Laser Polarimetry with Variable and Enhanced Corneal Compensation. *Ophthalmology* 2007;144:1259-65.
20. Mai TA, Reus NJ, Lemij HG. Structure-function relationship is stronger with enhanced corneal compensation than with variable corneal compensation in scanning laser polarimetry. *Invest Ophthalmol Vis Sci* 2007;48:1651-8.
21. Garway-Heath DF, Poinoosawmy D, Fitzke FW, Hitchings RA. Mapping the visual field to the optic disc in normal tension glaucoma eyes. *Ophthalmology* 2000;107:1809-15.
22. Choi J, Cho HS, Lee CH, Kook MS. Scanning laser polarimetry with variable corneal compensation in the area of apparently normal hemifield in eyes with normal tension glaucoma. *Ophthalmology* 2006;113:1954-60.
23. Reus NJ, Lemij HG. Relationships between standard automated perimetry, HRT confocal scanning laser ophthalmoscopy, and GDx-VCC scanning laser polarimetry. *Invest Ophthalmol Vis Sci* 2005;46:4182-8.
24. Bowd C, Zangwill LM, Weinreb RN. Association between scanning laser polarimetry measurements using variable corneal polarization compensation and visual field sensitivity in glaucomatous eyes. *Arch Ophthalmol* 2003;121:961-6.
25. Fedeiros FA, Zangwill LM, Bowd C, Weinreb RN. Comparison of the GDx-VCC scanning laser polarimeter, HRT II confocal scanning laser ophthalmoscope, and StratusOCT optical coherence tomography for the detection of glaucoma. *Arch Ophthalmo*l 2004;122:827-37.